Published OnlineFirst July 19, 2013; DOI: 10.1158/0008-5472.CAN-12-4593

Cancer Research

A Synthetic Lethality–Based Strategy to Treat Cancers Harboring a Genetic Deficiency in the Chromatin Remodeling Factor BRG1

Takahiro Oike, Hideaki Ogiwara, Yuichi Tominaga, et al.

Cancer Res 2013;73:5508-5518. Published OnlineFirst July 19, 2013.

Published OnlineFirst July 19, 2013; DOI: 10.1158/0008-5472.CAN-12-4593

Therapeutics, Targets, and Chemical Biology

Cancer Research

A Synthetic Lethality–Based Strategy to Treat Cancers Harboring a Genetic Deficiency in the Chromatin Remodeling Factor BRG1

Takahiro Oike[1,2,6], Hideaki Ogiwara[1], Yuichi Tominaga[3], Kentaro Ito[3], Osamu Ando[3], Koji Tsuta[4], Tatsuji Mizukami[1,6], Yoko Shimada[1], Hisanori Isomura[1,2], Mayumi Komachi[6], Koh Furuta[4], Shun-Ichi Watanabe[5], Takashi Nakano[6], Jun Yokota[2], and Takashi Kohno[1]

Abstract

The occurrence of inactivating mutations in SWI/SNF chromatin-remodeling genes in common cancers has attracted a great deal of interest. However, mechanistic strategies to target tumor cells carrying such mutations are yet to be developed. This study proposes a synthetic-lethality therapy for treating cancers deficient in the SWI/SNF catalytic (ATPase) subunit, BRG1/SMARCA4. The strategy relies upon inhibition of BRM/SMARCA2, another catalytic SWI/SNF subunit with a BRG1-related activity. Immunohistochemical analysis of a cohort of non–small-cell lung carcinomas (NSCLC) indicated that 15.5% (16 of 103) of the cohort, corresponding to preferentially undifferentiated tumors, was deficient in BRG1 expression. All BRG1-deficient cases were negative for alterations in known therapeutic target genes, for example, *EGFR* and *DDR2* gene mutations, *ALK* gene fusions, or *FGFR1* gene amplifications. RNA interference (RNAi)–mediated silencing of *BRM* suppressed the growth of BRG1-deficient cancer cells relative to BRG1-proficient cancer cells, inducing senescence via activation of p21/CDKN1A. This growth suppression was reversed by transduction of wild-type but not ATPase-deficient BRG1. In support of these *in vitro* results, a conditional RNAi study conducted *in vivo* revealed that BRM depletion suppressed the growth of BRG1-deficient tumor xenografts. Our results offer a rationale to develop BRM-ATPase inhibitors as a strategy to treat BRG1/SMARCA4–deficient cancers, including NSCLCs that lack mutations in presently known therapeutic target genes. *Cancer Res; 73(17); 5508–18. ©2013 AACR.*

Introduction

Tyrosine kinase inhibitors are effective against solid tumors with activating mutations in tyrosine kinase genes, for example, the *EGFR* mutations and *ALK* fusions harbored by lung adenocarcinomas (1). We and others recently identified *RET* oncogene fusions in lung adenocarcinoma (2–4), supporting the importance of tyrosine kinase genes as therapeutic targets. Two other tyrosine kinase gene alterations, the *FGFR1* amplification and the *DDR2* mutation, have been identified as therapeutic targets in squamous cell carcinoma, which corresponds to another major type of non–small-cell lung carcinoma (NSCLC; refs. 5, 6). Meanwhile, inactivating somatic mutations of genes that encode subunits of the SWI/SNF chromatin-remodeling complex, such as *BRG1/SMARCA4*, *PBRM1/BAF180*, *ARID1A/BAF250A*, and *ARID2/BAF200*, have attracted much interest as they were first identified by genome-wide sequencing analyses of cancer cells (7). Such mutations are thought to interfere with the functions of the SWI/SNF complex in transcription (7) and DNA double-strand break repair (8), which are likely to be critical for cancer development and/or progression. However, no therapeutic strategies have yet been developed for specifically targeting cancer cells harboring these inactivating *SWI/SNF* mutations.

Synthetic-lethality therapy holds great promise. The *BRCA1* and *BRCA2* genes have a synthetic-lethal relationship with the *PARP1* gene; the growth of *BRCA1*- or *BRCA2*-deficient cancer cells is dependent on PARP1 function. These findings have been translated to the clinic through the development of PARP inhibitors to treat *BRCA1/BRCA2*–deficient tumors (9). Synthetic-lethality therapy has also been proposed for treatment of cancers deficient in genes involved in DNA mismatch repair and cell metabolism (10–12). Here, we developed a novel synthetic-lethality strategy for killing tumor cells deficient in the SWI/SNF subunit BRG1 (also known as SMARCA4). Indeed, inactivating somatic *BRG1* mutations are present in several cancers, as reported by our group and others (13–15). Many lung cancers (10%–30%) exhibit reduced or absent expression

Authors' Affiliations: Divisions of [1]Genome Biology and [2]Multistep Carcinogenesis, National Cancer Center Research Institute; [3]Oncology Research Laboratories, Daiichi Sankyo Co., Ltd.; Divisions of [4]Pathology and Clinical Laboratories and [5]Thoracic Surgery, National Cancer Center Hospital, Tokyo; and [6]Department of Radiation Oncology, Gunma University Graduate School of Medicine, Gunma, Japan

Note: Supplementary data for this article are available at Cancer Research Online (http://cancerres.aacrjournals.org/).

Corresponding Author: Takashi Kohno, Division of Genome Biology, National Cancer Center Research Institute, 5-1-1 Tsukiji, Chuo-ku, Tokyo 104-0045, Japan. Phone: 81-3-3542-2511; Fax: 81-3-3542-0807; E-mail: tkkohno@ncc.go.jp

doi: 10.1158/0008-5472.CAN-12-4593

Published OnlineFirst July 19, 2013; DOI: 10.1158/0008-5472.CAN-12-4593

of the BRG1 protein due to somatic truncating mutations in the *BRG1* gene or unspecified epigenetic alterations (13, 15–18). Furthermore, *BRG1* was recently identified as one of the most frequently mutated genes in medulloblastoma (19, 20) and Burkitt lymphoma (21).

Each SWI/SNF complex contains either BRG1 or BRM (also known as SMARCA2) as its catalytic (ATPase) subunit (7, 22). BRG1 and BRM play complementary roles, as indicated by the observation that *Brm*-deficient mice develop normally but exhibit upregulated BRG1 expression in somatic cells (23). *Brg1*-null heterozygous mice spontaneously develop mammary tumors, and specific alleles of *BRG1* are associated with cancer predisposition in humans (24). Therefore, *BRG1/Brg1* acts as a tumor-suppressor gene (25). The complementary roles of BRG1 and BRM, coupled with the involvement of the SWI/SNF complex in multiple critical cellular functions, suggest that BRG1 and BRM might have a synthetic-lethal relationship; therefore, we examined the ability of BRM inhibition to specifically kill BRG1-deficient tumor cells. In addition, to address the potential significance of BRM-inhibitory therapies, we examined the characteristics of BRG1-deficient NSCLCs, including the mutually exclusive relationship between BRG1 deficiencies and mutations in therapeutic target genes (*EGFR* and *DDR2* mutations, *ALK* fusions, and *FGFR1* amplifications; Fig. 1A).

Materials and Methods

NSCLC cohort

Surgical specimens from 103 patients with NSCLC (51 adenocarcinomas and 53 squamous cell carcinomas), who received surgical resection at the National Cancer Center Hospital (Tokyo, Japan), between 1997 and 2007, were analyzed (Table 1 and Supplementary Materials and Methods). The study was approved by the Institutional Review Board of the National Cancer Center (Tokyo, Japan).

Immunohistochemical analysis of BRG1 and BRM

Immunohistochemical analysis was conducted on tissue microarray sections obtained from anonymized NSCLC samples. The methods used for immunohistochemical staining and the criteria for BRG1 and BRM positivity are described in the Supplementary Materials and Methods. Specific staining for BRG1 and BRM was confirmed by immunoblot analysis of cancer cell lines (Supplementary Fig. S1).

Examination of driver gene mutations

Genomic DNA obtained from tumor tissues was analyzed for somatic mutations in the *EGFR* and *KRAS* genes using the high-resolution melting method (26). Mutations in all *DDR2* coding regions in squamous cell lung carcinoma samples were examined by targeted genome capture and massively parallel sequencing using an Ion PGM sequencing system (Life Technologies) and the HaloPlex Target Enrichment System (Agilent Technologies). EML4-ALK and KIF5B-ALK fusions were screened by immunohistochemistry using an anti-ALK antibody (Abcam; 5A4), followed by confirmation via reverse-transcriptase PCR (RT-PCR) and/or fluorescence/chromogenic *in situ* hybridization (27). *RET* and *ROS1* fusions (in cases for which RNA samples are available) were examined by RT-PCR (2, 4). *FGFR1* amplification was examined by conducting FISH analysis (28) on 69 NSCLC samples that were available for analysis (Supplementary Materials and Methods).

Cell lines

A427, A549, H157, H460, H520, H522, H661, H1299, H1703, H1819, LK2, HCC515, II-18 (NSCLC), U2OS (osteosarcoma), HT1080 (fibrosarcoma), HeLa (cervical cancer), WiDr, HCT116 (colorectal cancer), HFL-1, and MRC-5 (fibroblast) cells were cultured in RPMI-1640 (Gibco) supplemented with 10% FBS. 293FT cells were cultured in Dulbecco's Modified Eagle Medium (DMEM) supplemented with 10% FBS. A549, H1819, H661, H157, H1299, A427, H522, and H1703 are lung cancer cell lines harboring truncating *BRG1* mutations, whereas H520, HeLa, LK2, H460, U2OS, and HT1080 carry wild-type BRG1 (13, 17). The *BRG1* mutation status of all the cell lines used in this study is given in Supplementary Table S1. Alterations in *BRG1* and other cancer-related genes were verified in the cell lines we examined; some of the results were previously reported (Supplementary Table S2; ref. 17).

Mutations in *BRG1*- and *BRM*-coding regions in HCC515 and II-18 cells, which do not express BRG1, and 16 primary tumors negative for BRG staining were examined by targeted genome capture and massively parallel sequencing of genomic DNA using an Ion PGM sequencing system and the Ion TargetSeq Custom Enrichment Kit (Life Technologies). Mutations detected were verified by Sanger sequencing of genomic PCR products. The effect of single-nucleotide variants resulting in amino acid changes in the BRG1 ATPase domain, expressed in HCT116 (L1163P) and WiDr (D1284N) colorectal cancer cells (16), was estimated using the PolyPhen and PolyPhen-2 programs. The substitutions in HCT116 cells are thought to abrogate ATPase activity, but those in WiDr cells are benign (Supplementary Table S3).

siRNA

ON-TARGET plus SMARTpool siRNA (Dharmacon) was used in this study. To knockdown the BRM protein, cells were transfected with siBRM (cat. no: 6597: SMARCA4) using Lipofectamine RNAiMAX (Invitrogen). Nontargeting siRNA (L-001810-10) was used as a negative control.

Establishment of cells expressing doxycycline-inducible short hairpin BRM

To achieve doxycycline-inducible knockdown of BRM, a lentiviral vector–based short hairpin RNA (shRNA)–mediated conditional gene-expression system [established by Wiznerowicz and Trono (29)] was used (Supplementary Materials and Methods). H1299 cells carrying a shRNA targeting *BRM* (H1299-shBRM) or shRNA targeting the *GFP* gene (H1299-shControl) were established. HeLa-shBRM and HeLa-shControl cells were established in the same manner.

Immunoblot analysis

Immunoblotting was conducted as previously described (8). The antibodies used in the present study are listed in the Supplementary Materials and Methods.

Published OnlineFirst July 19, 2013; DOI: 10.1158/0008-5472.CAN-12-4593

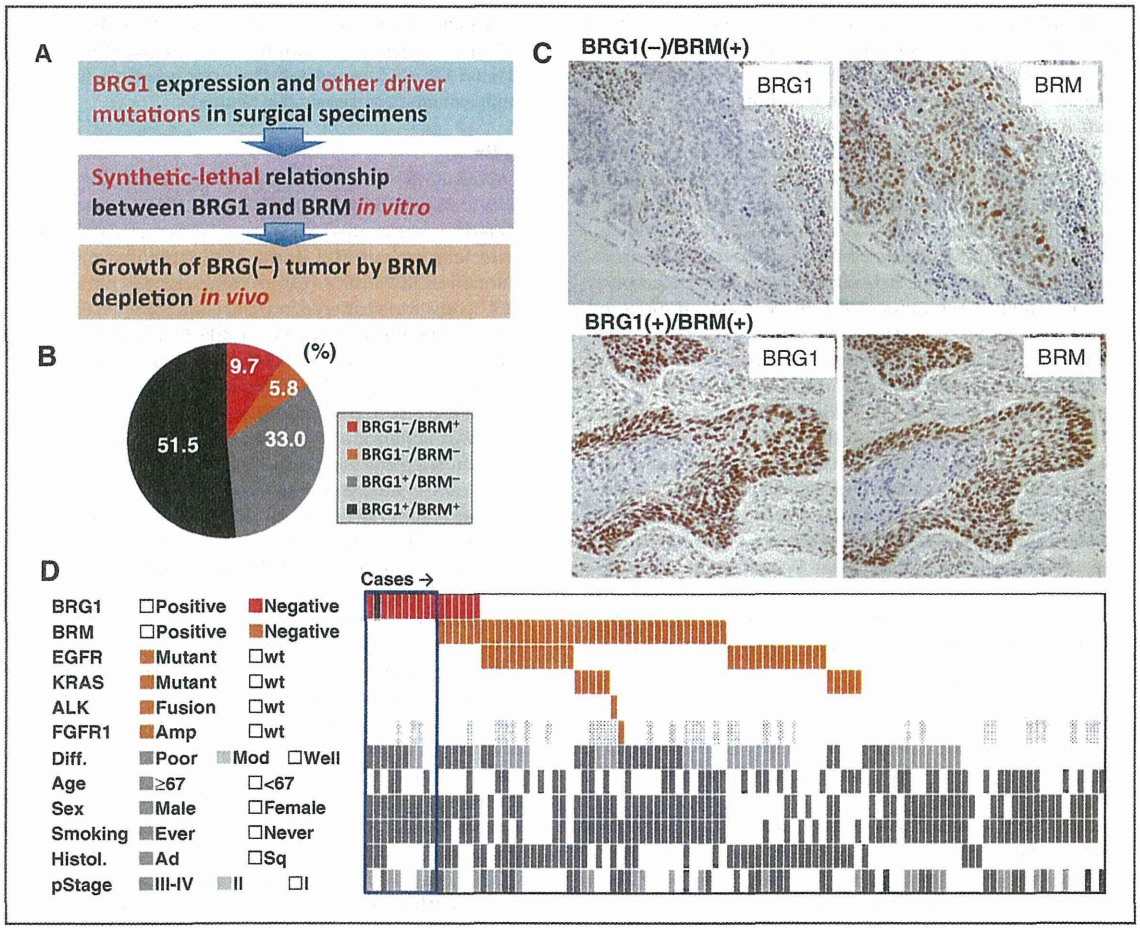

Figure 1. BRG1 and BRM expression in surgically resected NSCLCs. A, strategy. B, proportion of specimens expressing the BRG1 and BRM proteins. The staining intensity of BRG1 and BRM antibodies in the tumor cell nuclei in each lung cancer sample was scored according to Fukuoka and colleagues (46): 0, no signal; 1, weak; 2, moderate; and 3, strong; comparable with that in salivary gland cells used as the positive control; in addition, the intratumoral fractions of regions with each score (0–3) were determined. The total score for each lung cancer tissue (the sum of the intensity scores and the fractions) was compared with that of noncancerous lung tissues ($n = 6$). A tumor sample was judged positive (+) or negative/weak (−) when the total score was higher or lower, respectively, than the average total score of the normal lung epithelial tissues. C, representative images of immunohistochemical staining. Top, a BRG1-negative/BRM-positive specimen. Bottom, a BRG1/BRM–positive specimen. The stromal cells in both specimens were positive for BRG1 and BRM. D, BRG1/BRM protein expression and other clinicopathologic factors. Patients are characterized according to BRG1 and BRM staining and driver gene mutations. *BRG1*, a case of adenocarcinoma with a nonsense *BRG1* mutation is dotted. *FGFR1*, cases not examined for *FGFR1* amplification are dotted. *DDR2* mutations were not detected in all cases of squamous cell carcinoma. wt, wild-type.

Cell survival assay

The effect of BRM knockdown on the survival of BRG1-deficient (undetectable by immunoblot analysis) and BRG1-proficient (detectable by immunoblot analysis) cancer cells was evaluated using clonogenic survival assays. Because noncancerous fibroblasts do not form colonies on culture plates, the viability of these cells was determined by examining cellular ATP levels using the CellTiter-Glo Luminescent Cell Viability Assay Kit (Promega). The detailed procedures for these assays were described in the Supplementary Materials and Methods.

Complementation assay

The complementary role of BRG1 was examined in BRM-depleted cancer cells by transfecting cDNAs encoding wild-type and mutant BRG1 ($BRG1^{K785A}$, which disrupts the ATP-binding pocket in BRG1; ref. 30) into BRG1-null H1299 cells (Supplementary Materials and Methods).

Cell-cycle analysis

Cells were trypsinized, centrifuged, washed in PBS, and fixed in ice-cold 70% ethanol. The cells were then centrifuged again, incubated with PBS containing 200 μg/mL RNase A and

Published OnlineFirst July 19, 2013; DOI: 10.1158/0008-5472.CAN-12-4593

Table 1. Patient characteristics and their association with lost/reduced BRG1/SMARCA4 expression

Variant	All N (%)	BRG1 lost/reduced N (%)	BRG1 retained N (%)	*P* Univariate[a]	*P* Multivariate[b]
Total patients	103 (100.0)	16 (100.0)	87 (100.0)	NT	NT
Age					
Median [range] ± SD	67 [44–82] ± 8	60 [48–78] ± 8	67 [44–82] ± 8	0.094	0.13
>Median	52 (50.5)	5 (31.3)	47 (54.0)		
Gender					
Male	73 (70.9)	16 (100.0)	57 (65.5)	0.0053	NT
Female	30 (29.1)	0 (0.0)	30 (34.5)		
Histologic cell type					
Adenocarcinoma	50 (48.5)	8 (50.0)	42 (48.3)	0.90	NT
Squamous cell carcinoma	53 (51.5)	8 (50.0)	45 (51.7)		
Differentiation					
Well differentiated	38 (36.9)	2 (12.5)	36 (41.4)	0.0011	0.022
Moderately differentiated	34 (33.0)	3 (18.8)	31 (35.6)		
Poorly differentiated	31 (30.1)	11 (68.8)	20 (23.0)		
Pathologic stage					
I	42 (40.8)	5 (31.3)	37 (42.5)	0.078	0.20
II	28 (27.2)	8 (50.0)	20 (23.0)		
III and IV	33 (32.0)	3 (18.8)	30 (34.5)		
Smoking habit					
Never-smoker	26 (25.2)	1 (6.3)	25 (28.7)	0.057	0.17
Ever-smoker	77 (74.8)	15 (93.8)	62 (71.3)		
EGFR mutation					
Mutant	27 (26.2)	0 (0.0)	27 (31.0)	0.0095	NT
Wild-type	76 (73.8)	16 (100.0)	60 (69.0)		
KRAS mutation					
Mutant	10 (9.7)	0 (0.0)	10 (11.5)	0.15	NT
Wild-type	93 (90.3)	16 (100.0)	77 (88.5)		
ALK fusion					
Positive	1 (1.0)	0 (0.0)	1 (1.1)	0.67	NT
Negative	102 (99.0)	16 (100.0)	86 (98.9)		
FGFR1 amplification					
Positive	1 (1.0)	0 (0.0)	1 (1.1)	0.67	NT
Negative	68 (99.0)	12 (100.0)	56 (98.9)		
BRM expression					
Lost or reduced	40 (38.8)	6 (37.5)	34 (39.1)	0.91	NT
Retained	63 (61.2)	10 (62.5)	53 (60.9)		

Abbreviation: NT, not tested.

[a]Association was examined by Fisher exact test.

[b]Association was examined by logistic regression test. Variables showing associations with $P < 0.1$ in the univariate analysis were subjected to this analysis. Gender and *EGFR* mutation were not included; they are not suitable for this analysis because no females or *EGFR* mutants were present in the "BRG lost/reduced" group.

5 μg/mL propidium iodide, and analyzed for cell-cycle distribution by Guava flow cytometry (Millipore).

Senescence-associated β-galactosidase staining

Senescence-associated β-galactosidase (SA-β-gal) staining was conducted using the Senescence β-Galactosidase Staining Kit (Cell Signaling Technology). The percentage of SA-β-gal–positive cells was determined from three different fields per sample.

Fluorescence microscopy

Cells were stained with 4′,6-diamidino-2-phenylindole (DAPI) and examined for senescence-associated heterochromatic foci (SAHF) and signs of mitotic catastrophe (Supplementary Materials and Methods).

Long-term *in vitro* cell proliferation assay

H1299-shBRM and HeLa-shBRM cells were seeded in 60-mm dishes (1×10^5 cells/dish) in media with or without 0.1 μg/mL

Published OnlineFirst July 19, 2013; DOI: 10.1158/0008-5472.CAN-12-4593

doxycycline, and then cultured. The cells were trypsinized and counted every 3 days, and after each count, 1×10^5 cells were reseeded in new dishes with fresh medium. Accumulated cell numbers were calculated at each passage, based on the total number of cells and the dilution ratio at the time of passage. The experiment was carried out in duplicate.

Mouse xenograft model

The effect of *BRM* ablation on the growth of H1299-shBRM and H1299-shControl tumor xenografts was examined in BALB/c-nu/nu mice (Supplementary Materials and Methods). All experiments were approved by the Ethical Committee on Animal Experiments at the National Cancer Center.

Statistical analysis

Logistic regression analysis was conducted using JMP (ver 5.1). Fisher exact test and Student *t* test were conducted using StatMate III (ver 3.17). $P < 0.05$ was considered statistically significant. Experiments were carried out in triplicate unless otherwise stated.

Results

Characteristics of BRG1-deficient NSCLCs

We first examined the characteristics of BRG1-deficient NSCLCs. Because BRG1 has been reported to play a role in cell differentiation (31), the examined cases were selected to include similar numbers of adenocarcinomas and squamous cell carcinomas of the three differentiation grades (well, moderately, and poorly differentiated; Table 1). This approach allowed an efficient analysis of the association between BRG1 expression and tumor differentiation. Immunohistochemical analysis revealed that BRG1 protein expression was either low or absent in 16 of 103 (15.5%) NSCLCs (Fig. 1B and C). Low or absent BRG1 expression was more prevalent in poorly differentiated tumors (Table 1 and Fig. 1D), and was also prevalent in males and smokers. Mutational analysis of *BRG1* and *BRM* in 16 cases negative for BRG1 staining revealed that 1 case had nonsense *BRG1* mutations (Supplementary Fig. S2), whereas the remaining 15 did not, implying that both genetic alterations and epigenetic silencing of the *BRG1* gene can cause BRG1 deficiency, as previously reported (18). On the other hand, deleterious *BRM* mutations were not detected in these 16 cases including 5 that were negative for BRM staining.

Driver gene mutations in BRG1-deficient NSCLCs

Next, we analyzed representative therapeutically relevant gene mutations (*EGFR* and *KRAS* gene mutations and *ALK* fusions) in the 103 NSCLC cases. The 16 BRG1-deficient cases were negative for mutations in all three driver genes, including the two therapeutic targets (*EGFR* mutation and *ALK* fusion; Fig. 1D, Table 1). We also analyzed other driver gene mutations, *RET* and *ROS1* fusions (2–4), in the 9 BRG1-deficient cases for which tumor tissue RNA was available, but we detected no fusions. Recent whole-genome analyses have also suggested that *BRG1* mutations are prevalent in tumors without *EGFR* mutations or *ALK* fusions (Supplementary Table S4; refs. 32, 33). In addition, all the BRG1-deficient cases were also negative for two other alterations, *FGFR1* amplifications and *DDR2* mutations (Fig. 1D; Table 1; Supplementary Fig. S3; refs. 5, 6). These findings suggest that most BRG1-deficient NSCLCs are not suitable for current molecularly targeted therapies based on tyrosine kinase inhibitors (1). Of the 16 BRG1-deficient cases, 10 (62.5%, 9.7% of all cases studied) expressed BRM.

BRM-dependent growth of BRG1-deficient cancer cells

We then compared the effect of siRNA-mediated *BRM* ablation on *in vitro* growth of BRG1-deficient ($n = 10$) and BRG1-proficient ($n = 8$) cancer cell lines, using a clonogenic survival assay (Fig. 2A). Most (8 of 10) *BRG1*-deficient cells carry truncating *BRG1* mutations/deletions (Supplementary Table S2; refs. 13, 17). Of the remaining two BRG1-deficient cell lines, we detected a homozygous nonsense mutation in one (HCC515) by targeted genome capture sequencing (Supplementary Fig. S2), but no *BRG1* mutation in the other (II-18). On the other hand, BRG1-proficient cancer cells did not harbor such deleterious *BRG1* mutations (except HCT116 cells, which harbor a heterozygous missense mutation that is likely to disrupt the BRG1 ATPase domain; ref. 15).

We observed suppression of colony formation in all BRG1-deficient cells tested, but not in BRG1-proficient lines other than HCT116 (Fig. 2B and C). The mean values of the surviving fraction of cancer cell lines are summarized according to the BRG1 and BRM expression status in Fig. 2D. Survival of BRG1-deficient cells upon BRM knockdown was significantly lower than that of BRG1-proficient lines ($P = 6.3 \times 10^{-6}$ by Student *t* test). The BRM protein was undetectable, or detectable only at trace levels, in three BRG1-deficient cell lines, A427, H522, and H1703 (Fig. 2A and Supplementary Fig. S4A). These findings are consistent with a report showing that a fraction of lung cancer cells lack, or express at low levels, both BRG1 and BRM (Fig. 1B; ref. 14). Conceivably, the effect of siRNA-mediated BRM knockdown in these three cell lines was less evident than in the other seven. Thus, among BRG1-deficient cell lines, the suppression of colony formation by BRM knockdown was more prominent in cell lines that originally expressed the BRM protein ($P = 4.5 \times 10^{-9}$ by Student *t* test; Fig. 2D).

BRM knockdown did not affect the growth of the noncancerous fibroblast cell lines HFL-1 and MRC-5, which express both BRG1 and BRM (Fig. 3A and B). Wild-type *BRG1* cDNA complemented the sensitivity of BRG1-deficient H1299 cells to *BRM* siRNA-mediated growth inhibition (Fig. 3C and D), whereas cDNA of an ATPase mutant with a disrupted ATP-binding pocket, $BRG1^{K785A}$ (30), did not ($BRG1^{K785A}$ is indicated as KA in Fig. 3C and D). These results indicated that BRG1-deficient cancer cells depend on BRM for growth, and that this phenotype is caused by a lack of BRG1 ATPase activity.

BRM depletion induces senescence in BRG1-deficient cancer cells

To examine the long-term effects of *BRM* depletion, we prepared H1299 (BRG1-deficient) and HeLa (BRG1-proficient) cells expressing either a doxycycline-inducible shRNA targeting *BRM* (H1299-shBRM and HeLa-shBRM; refs. 29, 34) or a nontargeting shRNA (H1299-shControl and HeLa-shControl). To confirm the effects of BRM knockdown, we used a different

Published OnlineFirst July 19, 2013; DOI: 10.1158/0008-5472.CAN-12-4593

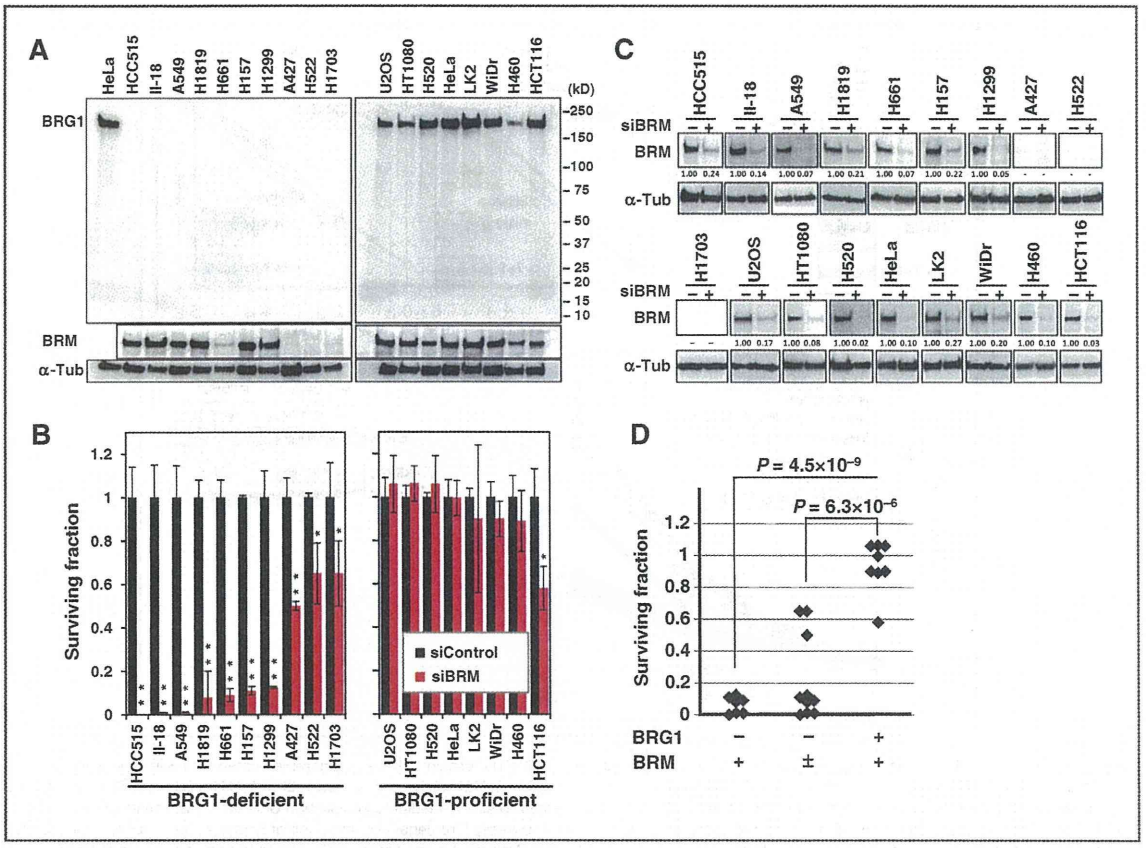

Figure 2. Differential sensitivity of BRG1-deficient and -proficient cell lines to BRM knockdown. A, BRG1 and BRM protein expression in human cancer cell lines. Immunoblot analysis of BRG1-deficient (left) and BRG1-proficient (right) cancer cell lines. Blots of whole-cell extracts were probed with antibodies against BRG1, BRM, and α-tubulin (α-Tub; loading control). B, survival of BRG1-deficient and -proficient cancer cells after BRM knockdown. BRG1-deficient (left) and -proficient (right) cells were transfected with *BRM*-targeting siRNA (siBRM) or nontargeting siRNA (siControl) for 48 hours and then assayed for colony formation. The surviving fraction of siBRM-treated cells at 10 days was calculated as a ratio (number of colonies formed by siBRM-treated cells/number of colonies formed by siControl-treated cells). Data are shown as mean ± SD. Asterisks show significant differences in surviving fraction between siBRM- and siControl-treated cells, as determined by Student *t* test (*, $P < 0.05$; **, $P < 0.001$). C, BRM protein expression in cancer cells after siRNA-mediated knockdown. Cells were transfected with siBRM or siControl for 48 hours, harvested, and subjected to immunoblot analysis. Blots of whole-cell extracts were probed with antibodies against BRM and α-tubulin (loading control). The expression levels of BRM in siBRM-treated cells are shown relative to those in siControl-treated cells. Knockdown efficiency in A427, H522, and H1703 cells could not be assessed because of their low endogenous BRM expression levels. D, surviving fraction of cancer cell lines according to BRG1 and BRM expression status. The mean values of the surviving fractions of each cell line obtained in Fig. 2B are shown. Cell lines are grouped according to deficiency (–) and proficiency (+) of BRG1 and BRM protein expression. Significance of differences in the mean values of surviving fraction between BRG1-deficient cell lines and BRG1-proficient cell lines, and BRG1-deficient/BRM-proficient cell lines and BRG1-proficient cell lines were evaluated using Student *t* test.

BRM target site from the one used in the siRNA experiments. The results of the siRNA clonogenic assay were confirmed using this system (Supplementary Fig. S5). We next examined the mechanism underlying growth inhibition in H1299-shBRM cells. Seven days after doxycycline treatment, H1299-shBRM cells, but not HeLa-shBRM cells, exhibited G_1 arrest with an enlarged and flattened morphology, suggesting senescence (Fig. 4A and Supplementary Fig. S6). Biomarkers of senescence (p21/CDKN1A expression, SA-β-gal staining, and SAHF; refs. 35, 36) were observed in doxycycline-treated H1299-shBRM cells, but not in HeLa-shBRM cells (Fig. 4B and C). Doxycycline treatment did not affect the proportion of cells in sub-G_1-phase or the number of cells exhibiting distinct nuclear lobation, indicating that ablation of *BRM* does not induce apoptosis or mitotic catastrophe (Fig. 4A and C; ref. 37). Senescence is an irreversible state of growth arrest that is maintained by p21 (38); therefore, we examined p21 expression in H1299-shBRM cells in which BRM was reexpressed after doxycycline removal (Fig. 4D). In these cells, p21 expression was maintained at the level observed in BRM knockdown cells. Consistent with this, cells reexpressing BRM exhibited suppressed clonogenic growth activity. siRNA-mediated knockdown of BRM caused significant increases in SA-β-gal positivity and the number of cells in G_1-phase in three BRG1-deficient NSCLC cell lines

Published OnlineFirst July 19, 2013; DOI: 10.1158/0008-5472.CAN-12-4593

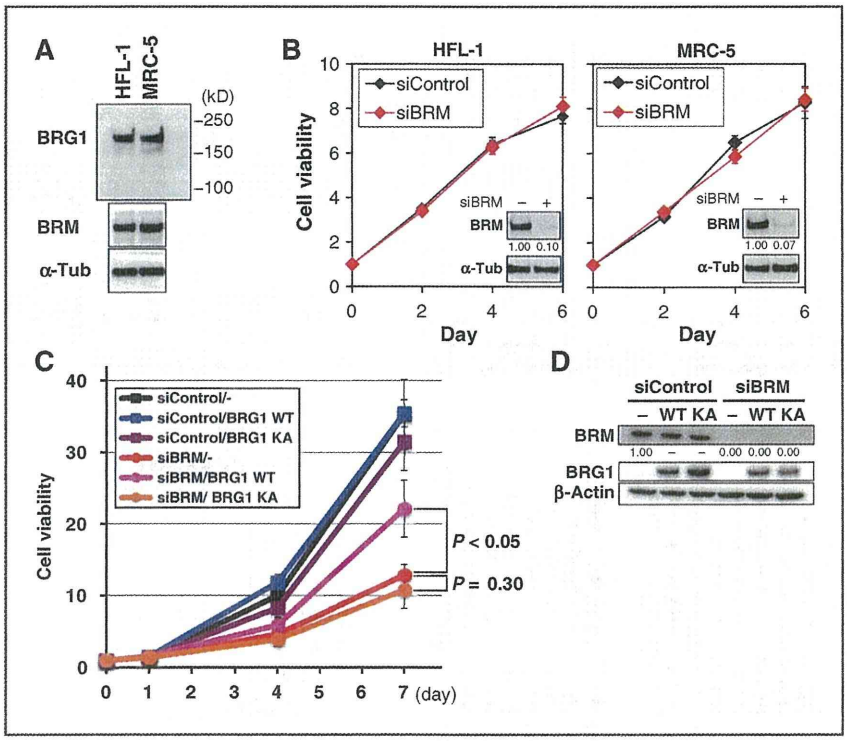

Figure 3. Effect of BRM knockdown on cell growth in noncancerous cells and in BRG1-deficient H1299 cells complemented with wild-type *BRG1* cDNA. A, BRG1 and BRM protein expression in HFL-1 and MRC-5 fibroblasts. Blots of whole-cell extracts were probed with antibodies against BRG1, BRM, and α-tubulin (α-Tub; loading control). B, viability of HFL-1 and MRC-5 cells subjected to siRNA-mediated knockdown of BRM. Cells transfected with siBRM or siControl were cultured for 48 hours and then subjected to CellTiter-Glo assay (Promega) and immunoblot analysis. Cell viability measured by CellTiter-Glo assay is expressed as a ratio relative to the viability assessed at day 0. Data are shown as mean ± SD. For immunoblot analyses, blots of whole-cell extracts were probed with antibodies against BRM and α-tubulin (loading control). The expression levels of BRM in siBRM-treated cells are shown relative to those in siControl-treated cells. C and D, *BRG1* cDNA complementation assay. Twenty-four hours after transfection with siBRM or siControl, H1299 cells were transfected with a plasmid expressing wild-type (WT) or ATPase-mutant (KA) BRG1 protein. Twenty-four hours later (day 0), the cells were seeded into a 96-well plate. On day 2, the cells were retransfected with siRNAs. Cell viabilities measured on days 0, 1, 4, and 7 are shown in C. *P* values were calculated using Student *t* test. Expression of BRM and BRG1 proteins on day 1, determined by immunoblot analysis, is shown in D. β-Actin was used as the loading control. The expression levels of BRM in siBRM-treated cells are shown relative to those in siControl-treated cells without cDNA complementation. Data are shown as mean ± SD of three replicates per treatment condition.

(H1299, A549, and H157), but not in three BRG1-proficient NSCLC cell lines (H520, LK2, and H460; Fig 4E–G; Supplementary Fig. S7). Taken together, these results suggest that BRM knockdown specifically suppresses the growth of BRG1-deficient cells by inducing senescence.

BRM-dependent growth of BRG1-deficient cancer cells *in vivo*

The number of *BRM*-depleted H1299-shBRM cells was approximately 1,000 times lower than that of nondepleted cells after 4 weeks of culture, whereas the number of HeLa-shBRM cells did not change (Fig. 5A). This observation suggests that inhibition of BRM specifically suppresses the long-term growth of *BRG1*-deficient cells (i.e., over at least a month). To further confirm these data under more physiologically relevant conditions, we introduced H1299-shBRM and H1299-shControl cells into an *in vivo* conditional RNA interference (RNAi) model (Fig. 5B). BALB/c-nu/nu mice were injected subcutaneously with H1299-shBRM or H1299-shControl cells. After 3 weeks, when the injected cells had formed tumor nodules measuring approximately 100 mm^3, the animals were randomly divided into two groups and fed a diet containing doxycycline (200 ppm) or a control diet for 1 month. In doxycycline-fed mice, the H1299-shBRM xenografts were significantly smaller than the H1299-shControl xenografts.

Discussion

This study suggests that *BRM* is a novel therapeutic target for synthetic-lethality therapy for BRG1-deficient cancers. To the best of our knowledge, this is the first report proposing a therapeutic strategy that specifically targets and kills cancer cells harboring inactivating mutations in SWI/SNF chromatin-remodeling genes. In the future, the use of this strategy needs to be further validated *in vivo* using multiple lines of BRG1-deficient and -proficient cancer cells.

Published OnlineFirst July 19, 2013; DOI: 10.1158/0008-5472.CAN-12-4593

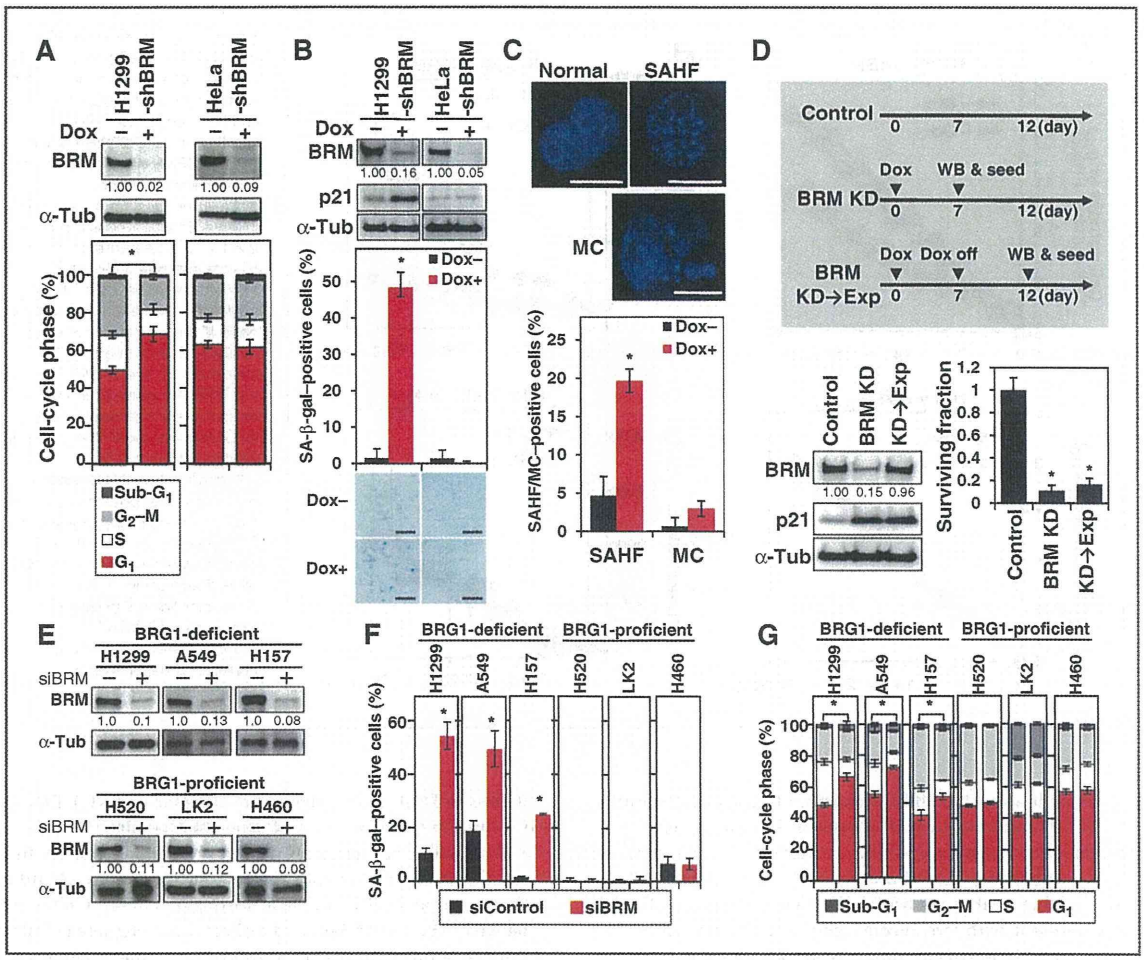

Figure 4. Effect of BRM knockdown on growth inhibition in BRG1-deficient cancer cells. A–D, H1299-shBRM and HeLa-shBRM cells were cultured in the presence or absence of doxycycline (Dox) for 7 days before analysis. H1299 cells carrying a doxycycline-inducible shRNA specific for GFP were used as a negative control (H1299-shControl). A, cell-cycle profile. Top, immunoblot analysis of BRM and α-tubulin (α-Tub). The expression level of BRM in doxycycline-treated cells is shown relative to the level in untreated cells. Bottom, cell-cycle profiles determined by flow cytometry. *, a significant difference in the fraction of cells in G_1-phase between doxycycline-treated and -untreated cells as determined by Student *t* test ($P < 0.01$). B, expression of SA-β-gal and p21. Top, immunoblot analysis of BRM, p21, and α-tubulin. The expression level of BRM in doxycycline-treated cells is shown relative to that in untreated cells. Middle, percentage of SA-β-gal–positive cells. *, a significant difference in the percentage of SA-β-gal–positive cells between doxycycline-treated and -untreated cells as determined by Student *t* test ($P < 0.001$). Bottom, representative micrographs showing cells stained for SA-β-gal (blue). Scale bars, 100 μm. C, SAHF and mitotic catastrophe (MC) as revealed by nuclear DAPI staining. Top, representative images showing normal nuclear (Normal), SAHF, and mitotic catastrophe patterns in doxycycline-treated H1299-shBRM cells. Scale bars, 10 μm. Bottom, percentage of cells exhibiting SAHF and mitotic catastrophe. *, a significant difference in the percentage of SAHF-positive cells between doxycycline-treated and -untreated cells as determined by Student *t* test ($P < 0.001$). D, p21 expression and clonogenic survival of H1299 cells after BRM knockdown followed by reexpression of BRM. A schematic of the experimental protocol is shown at the top. H1299-shBRM cells were cultured in the presence of doxycycline for 7 days (BRM KD) and then cultured in the absence of doxycycline for an additional 5 days (KD→Exp). The cells were then harvested and subjected to immunoblot analysis (WB). BRM KD and KD→Exp cells were seeded and cultured for an additional 10 days in the presence or absence of doxycycline, respectively, to allow colony formation. H1299-shBRM cells cultured in the absence of doxycycline were used as a control. Bottom left, immunoblot analysis of BRM, p21, and α-tubulin. The expression levels of BRM in BRM KD cells and KD→Exp cells are shown relative to the level in control cells. Bottom right, clonogenic survival assay. The surviving fraction of BRM KD and KD→EXP cells is expressed as a ratio (number of colonies formed by BRM KD and KD→EXP cells/number of colonies formed by control cells). Data are shown as mean ± SD. *, significant decreases in the surviving fraction relative to that of control cells as determined by Student *t* test ($P < 0.001$). E–G, BRG1-deficient (H1299, A549, and H157) and BRG1-proficient (H520, LK2, and H460) NSCLC cells were transfected twice (days 1 and 3) with *BRM*-targeting siRNA (siBRM) or nontargeting siRNA (siControl). On day 7, the cells were subjected to subsequent analyses. E, immunoblot analysis of BRM and α-tubulin (loading control). The expression levels of BRM in siBRM-treated cells are shown relative to those in siControl-treated cells. F, positivity for SA-β-gal staining. *, significant differences in the percentage of SA-β-gal–positive cells between siBRM-treated and siControl-treated cells as determined by Student *t* test ($P < 0.005$). G, cell-cycle profiles determined by flow cytometry. *, significant differences in the fraction of cells in G_1-phase between siBRM-treated and siControl-treated cells, as determined by Student *t* test ($P < 0.005$).

Published OnlineFirst July 19, 2013; DOI: 10.1158/0008-5472.CAN-12-4593

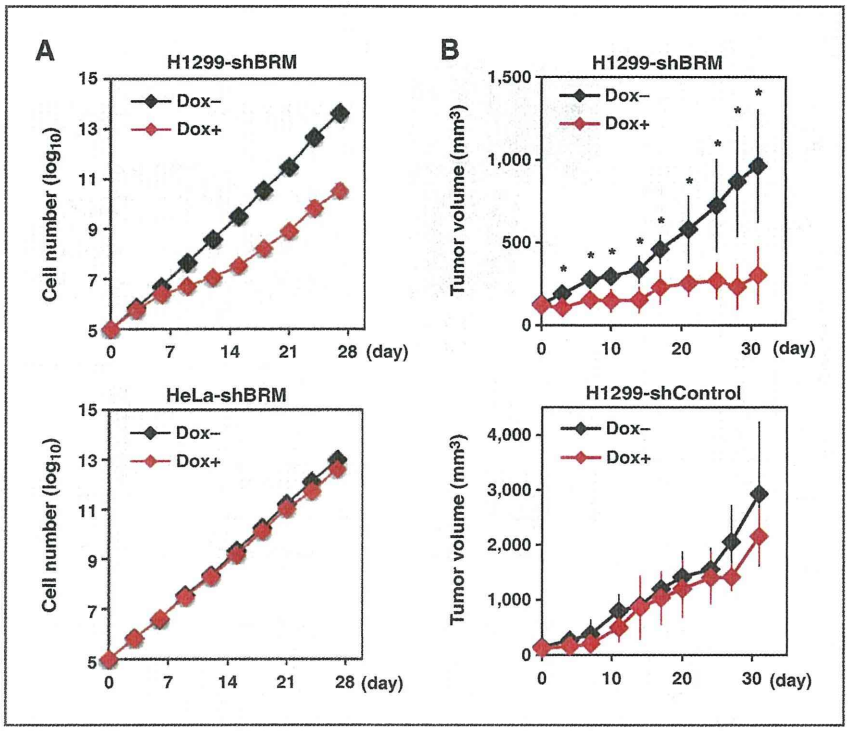

Figure 5. Suppression of BRG1-deficient cancer cell growth by BRM knockdown both *in vitro* and *in vivo*. A, long-term proliferation of H1299 and HeLa cells after BRM knockdown. H1299-shBRM and HeLa-shBRM cells were cultured in the presence or absence of doxycycline (Dox) for 4 weeks. The cells were trypsinized and counted, and 1×10^5 cells were reseeded into 60-mm dishes and given fresh medium every 3 days. Accumulated cell numbers were calculated on the basis of the cell number at each passage. B, growth of H1299 xenografts in mice. H1299-shBRM and H1299-shControl cells were implanted subcutaneously into BALB/c-nu/nu mice. After 3 weeks (when the tumors reached 100 mm^3), the mice were randomly divided into two groups and either fed a diet containing doxycycline (Dox+) or a control diet (Dox–). Tumors were measured twice per week. Data represent the mean ± SD. *, significant differences in the tumor volume between the doxycycline-fed mice and the controls, as determined by Student *t* test ($P < 0.05$).

In our cohort, all the BRG1-deficient tumors were negative for *EGFR* mutations and *ALK* fusions, both of which can be targeted by existing molecular therapies using tyrosine kinase inhibitors (1). This negative association of *BRG1*-inactivating mutations with therapeutic target mutations is consistent with two recent genome-wide mutation analyses of lung adenocarcinoma (Supplementary Table S4; refs. 32, 33). Indeed, *BRG1*-deficient NSCLC cell lines are resistant to tyrosine kinase inhibitors that target EGFR (e.g., A549, H1819, and H1299; ref. 39) or ALK (A549; ref. 40). Furthermore, those BRG1-deficient tumors were also negative for *FGFR1* amplifications and *DDR2* mutations, potential therapeutic targets recently identified in squamous cell lung carcinoma (5, 6). These findings highlight the importance of establishing a treatment strategy for targeting BRG1-deficient tumors. BRG1 and BRM proteins have ATPase activities and function as helicases to alter chromatin structure. ATPases are a druggable target (41); therefore, BRM-targeting therapy using specific inhibitors is a promising treatment of lung cancers that are not amenable to existing molecularly targeted therapies (1). To the best of our knowledge, specific pharmacologic inhibitors against ATPases involved in chromatin remodeling have not been developed; therefore, we are currently seeking to identify substrates that inhibit BRM-ATPase activity.

The results of this study show that BRG1 and BRM have a synthetic-lethal relationship. BRG1 functions as a key enzyme in SWI/SNF chromatin remodeling during transcription, as well as in DNA double-strand break repair (7, 8, 31). BRG1 is involved in the expression of genes that regulate cell growth and stem-cell properties. However, a preliminary study indicated that the expression of representative genes, including those encoding E2F1 and cyclin D1, does not differ significantly between BRG1-proficient and -deficient cells depleted of BRM. Thus, the mechanisms underlying the synthetic-lethal relationship between BRG1 and BRM remain unknown. Of concern is the subset of NSCLC cases (5.8%; Fig. 1B) that lack both BRG1 and BRM expression (14, 22, 42). BRM deficiency is likely to be due to epigenetic alterations as previously reported (43). The existence of these cases suggests that a portion of BRG1-deficient tumors will not respond well to therapies that target BRM, as suggested by our experiment using cancer cell lines (Fig. 2B). Such tumors may have acquired the ability to maintain cell growth through complementation by chromatin-remodeling proteins other than BRG1 and BRM, although our preliminary analysis did not reveal complementation by overexpression of other SWI/SNF and chromatin-remodeling proteins (Supplementary Fig. S4B). Studies of the molecular mechanisms underlying the maintenance of cell growth in the absence of both BRG1 and BRM would be valuable, because it is possible that BRG1-deficient cells could acquire resistance to *BRM*-targeted therapy.

The pathogenic significance of inactivating somatic mutations in genes encoding the subunits of the SWI/SNF chromatin-remodeling complex in human cancers is largely unknown (7). This study sheds light on this issue by showing